Acta Med. Okayama, 2018
Vol. 72, No. 2, pp. 165–174

Acta Medica Okayama
http://escholarship.lib.okayama-u.ac.jp/amo/

Original Article

Clinical and Functional Significance of Intracellular and Extracellular *microRNA-25-3p* in Osteosarcoma

Aki Yoshida[a], Tomohiro Fujiwara[a]*, Koji Uotani[a], Takuya Morita[a], Masahiro Kiyono[a], Suguru Yokoo[a], Joe Hasei[a], Eiji Nakata[a], Toshiyuki Kunisada[a,b], and Toshifumi Ozaki[a]

Departments of [a]Orthopaedic Surgery, [b]Medical Materials for Musculoskeletal Reconstruction, Okayama University Graduate School of Medicine, Dentistry and Pharmaceutical Sciences, Okayama 700-8558, Japan

Although there is considerable evidence indicating that the dysregulation of microRNAs (miRNAs) in malignant tumors plays a role in tumor development, the overall function of miRNAs and their clinicopathological significance are not well understood. In this retrospective analysis of 45 biopsy specimens from osteosarcoma (OS) patients, we investigated the functional and clinical significance of *miR-25-3p* in OS, which we previously identified as a highly expressed miRNA in OS patients' serum. We observed that *miR-25-3p* dysregulation in human OS tissues was negatively correlated with the clinical prognosis, whereas the expression level of its target gene, *Dickkopf WNT Signaling Pathway Inhibitor 3* (*DKK3*), was positively correlated with the clinical prognosis. Endogenous *miR-25-3p* upregulation promoted tumor growth, invasion, and drug resistance, which was consistent with *DKK3* silencing in OS cells. In addition, secretory *miR-25-3p* was embedded in tumor-derived exosomes, where it promoted capillary formation and the invasion of vascular endothelial cells. Overall, our results show that *miR-25-3p* has intracellular and extracellular oncogenic functions as well as clinicopathological relevance in OS, indicating its potential as a novel diagnostic and therapeutic tool for the clinical management of this disease.

Key words: microRNA, circulating microRNA, osteosarcoma, prognosis

Osteosarcoma (OS) is the most common primary malignant bone tumor, and occurs mainly in children and adolescents [1]. Historically, the clinical prognosis of OS improved significantly in the 1970s, with the survival rate reaching 60-70% after the advent of high-dose, multi-agent chemotherapy. However, survival measures have failed to demonstrate any further improvements in the prognosis of OS for more than 30 years, despite advances in surgical techniques and changes in chemotherapy regimens [2,3]. To date, there are few useful biomarkers for monitoring tumor burden and response to treatment in OS. Salvage chemotherapy is of limited efficacy, even after identifying relapse [2]. The development of diagnostic and therapeutic strategies based on a thorough understanding of the molecular basis of metastasis is thus required to improve patient survival.

MicroRNAs (miRNAs), a class of small noncoding RNAs, are involved in the post-translational regulation of gene expression via their ability to inhibit the stability and translation of messenger RNA (mRNA) [4]. miRNAs play important roles in a variety of physiological and pathological processes by modulating the expres-

Received October 31, 2017; accepted November 27, 2017.
*Corresponding author. Phone: +81-86-235-7273; Fax: +81-86-223-9727
E-mail: tomomedvn@gmail.com (T. Fujiwara)

Conflict of Interest Disclosures: No potential conflict of interest relevant to this article was reported.

sion of their multiple target genes [4,5]. To date, miRNA dysregulation has been documented in malignant tumors, demonstrating that miRNAs can have either an oncogenic or tumor suppressive function [6,7]. In addition, miRNAs were recently demonstrated to be secreted into the circulation in a cell-free form [8,9].

Despite the presence of RNase activity in human blood, circulating miRNAs are detectable in extracellular vesicles such as exosomes, which are secreted from tumor cells and play a biological and pathological role in intercellular communication within the tumor microenvironment and promote cell motility and invasion in cancer [10]. The demonstration of circulating miRNA levels in the blood or urine of patients may present a novel approach to predicting clinical behavior and therapeutic responses [9,11]. We previously identified the secretion of the miRNA *miR-25-3p* in OS cells, and *miR-25-3p* was also detected in the serum of OS patients [12]. Serum *miR-25-3p* at the pretreatment status *miR-25-3p* levels of the OS patients were significantly correlated with patient prognosis [12].

However, the clinicopathological significance and intracellular and extracellular functions of *miR-25-3p* dysregulation in OS have been unclear, and few reports have documented the functional and clinical value of *miR-25-3p* in the management of malignant tumors. In the present study, we investigated the functional and clinicopathological significance of intracellular and extracellular *miR-25-3p* dysregulation in OS toward an understanding of the overall function of *miR-25-3p* in tumor progression.

Materials and Methods

Human tissues. The study protocol was approved by the Institutional Review Board of Okayama University Hospital (No. 1509-037). All patients provided written, informed consent authorizing the collection and use of their samples for research purposes. Tumor samples from OS patients were collected between 2000 and 2015 at the Okayama University Hospital.

Cell lines and cell culture. The human OS cell lines 143B and U2OS were purchased from the American Type Culture Collection (Manassas, VA, USA). Human mesenchymal stem cells (hMSCs) were purchased from Lonza (Walkersville, MD, USA). Human umbilical vein endothelial cells (HUVECs) were purchased from PromoCell (Heidelberg, Germany). 143B and U2OS cells were cultured in Dulbecco's modified Eagle's medium (DMEM) (Life Technologies, Grand Island, NY, USA). All media were supplemented with 10% fetal bovine serum (FBS; Life Technologies), 50 units/ml penicillin, and 50 μg/ml streptomycin (Life Technologies). Cells were maintained under 5% CO_2 in a humidified incubator at 37°C.

Exosome isolation. Exosomes were purified from the culture medium supernatant as described previously [14]. The supernatant was ultracentrifuged using an Optima TL-100 ultracentrifuge (Beckman Coulter, Fullerton, CA, USA) at 110,000 g for 70 min to pellet the exosomes. The pellet was washed in phosphate-buffered saline (PBS) to eliminate contaminating proteins, and centrifuged again at 110,000 g for 70 min. The PBS was removed and the exosomes were re-suspended in 100 μl of PBS.

RNA extraction and RT-PCR. Total RNA (including miRNA) was extracted using an miRNeasy mini Kit (Qiagen, Valencia, CA, USA) according to the manufacturer's instructions. RNA samples were reverse transcribed using the TaqMan MicroRNA Reverse Transcription Kit (Applied Biosystems, Foster, CA, USA). For mRNA detection, total RNA was reverse transcribed using a PrimeScript RT Reagent Kit (Takara, Tokyo, Japan) according to the manufacturer's protocol. Quantitative polymerase chain reaction (PCR) was performed on an Agilent Mx3000P QPCR System (Agilent Technologies, Santa Clara, CA, USA) using TaqMan 2×Universal PCR Master mix and each primer. Data obtained from RT-PCR were analyzed using the $2^{-\Delta\Delta Ct}$ method. The miRNA expression levels were normalized using the miRNA cel-miR-39 for exosomes and the small non-coding RNA RNU6B for tumor cells, and the mRNA expression levels were normalized using GAPDH.

Western blots. Total protein was extracted from the cells using Mammalian Protein Extraction Buffer (GE Healthcare, Chicago, IL, USA). Fifteen μg of each protein extract was separated on Mini-PROTEAN® TGX gels (Bio-Rad Laboratories, Hercules, CA, USA) and transferred onto Immun-Blot® PVDF membranes (Bio-Rad). The membranes were probed with the following primary antibodies: anti-CD9 mouse monoclonal antibody (Abcam, Cambridge, UK), anti-CD81 mouse monoclonal antibody (Santa Cruz Biotechnology,

Santa Cruz, CA, USA), anti-β-actin mouse monoclonal antibody (Sigma-Aldrich, St. Louis, MO, USA), and anti-DKK3 rabbit polyclonal antibody (Abcam). The secondary antibody was IRDye® 800CW anti-rabbit IgG or IRDye® 680RD anti-mouse IgG (LI-COR, Lincoln, NE, USA).

Transfection with synthetic miRNAs, LNAs, and siRNAs. Synthetic hsa-miRs (pre-miR-hsa-miR-25 and negative control; Life Technologies) and locked nucleic acids (LNAs) (LNA-antimiR-25-3p and scramble control; Gene Design, Ibaraki, Japan) were transfected at a final concentration of 30 nM each with the use of the transfection agent DharmaFECT 1 (GE Healthcare). Synthetic siRNAs (Life Technologies) were transfected into the cells at a final concentration of 10 nM each using DharmaFECT 1 (GE Healthcare).

Prediction of miRNA target genes. The miRNA analysis web (http://www.microrna.org/) was used to identify candidate miRNAs. This web-based tool is integrated with three of the most commonly used target gene prediction algorithms: miRanda, MiRtarget2 and TargetScan.

Cell proliferation and cytotoxicity assays. Cell proliferation rates and cell viability were used as indicators of the relative sensitivity of the cells to doxorubicin, cisplatin, methotrexate, and docetaxel. Measurements were determined using the WST-1 Proliferation Assay (Sigma-Aldrich) per the manufacturer's instructions. Cells were seeded in 96-well plates after 24-h transfection, and treated with varying doses of doxorubicin (Sigma-Aldrich), cisplatin (Enzo Life Sciences, Farmingdale, NY, USA), methotrexate (Sigma-Aldrich), or docetaxel (Sigma-Aldrich) for 72 h. Absorbance was measured at 450 nm with a reference wavelength at 630 nm by a microplate reader (Bio-Rad). The relative number of viable cells is expressed as the percent of viable cells.

Cell migration and invasion assay. Cell invasion and migration were examined with 24-well BD BioCoat invasion chambers with and without Matrigel matrix (BD Biosciences, San Jose, CA, USA). Cells of the lines 143B, U2OS and HUVECs were trypsinized and seeded in chambers 48 h after transfection. The cells were subsequently suspended in medium without FBS and added to the upper chamber. Medium with 10% FBS was added to the lower chamber. After a 24-h incubation, the cells on the upper side were removed, and the filters were fixed in methanol and stained with Hemacolor® solution 3 (Merck, Darmstadt, Germany). The number of cells was counted in 6 separated high-power fields.

Luciferase assay. First, 143B cells were cotransfected with the pGL3-DKK3-3' untranslated region (UTR) or with the pGL3-DKK3-3'UTR Mut plasmid, the phRL-SV40 control vector (Promega, Fitchburg, WI, USA), and 30 nM *miR-25-3p* mimic or AccuTarget™ miRNA mimic negative control #1 (Bioneer, Alameda, CA, USA) using Lipofectamine® 3000 (Invitrogen, Waltham, MA, USA). After transfection for 48 h, we determined the renilla and firefly luciferase activities using a Dual Luciferase Reporter Gene Assay kit (Promega) according to the manufacturer's instructions. Luciferase activity was detected by a FlexStation 3 microplate reader (Molecular Devices, Sunnyvale, CA, USA). The firefly luciferase activity of each sample was normalized using the renilla luciferase activity.

Immunohistochemistry. Slides were heated for antigen retrieval in 10 mM sodium citrate (pH 6.0), followed by incubation with polyclonal goat anti-human DKK3 (Abcam) or isotype-matched control antibodies overnight at 4°C. Immunodetection was performed using Histofine anti-goat IgG (Nichirei, Tokyo, Japan) and the DAB substrate kit (Nichirei) according to the manufacturer's instructions. Sections were counterstained with hematoxylin to create contrast. The immunohistochemical (IHC) score was defined as the proportion of tumor cells with stained cell membrane: negative, 0-49%; focal, 50-79%; diffuse, 80-100%.

Tube formation assay. HUVECs were plated on top of Matrigel and treated with exosomes (50 ng per well) derived from OS cells 48 h after transfection. Tube formation was quantified by counting the branch point number in three wells after 24 h. The average number of each group was calculated and normalized to the average number of the control group.

Statistical analysis. Experiments were repeated at least 3 times. Statistical analyses were performed using SPSS ver. 23 software (SPSS, Chicago, IL, USA). Student's two-tailed *t*-test was used for comparisons of pairs of groups. For comparisons of more than 2 groups, we performed a one-way analysis of variance (ANOVA). The differences in *miR-25-3p* expression among different clinicopathological data were analyzed by the chi-squared test. The Kaplan-Meier method and the log-rank test were used to compare the survival of patients. P-values < 0.05 were considered significant.

Results

The dysregulated miR-25-3p expression levels in OS tissue specimens were negatively correlated with the patient prognosis. To investigate the clinical significance of *miR-25-3p* expression levels in OS tissue specimens, we performed a Kaplan-Meier analysis on the RT-PCR results of 45 fresh frozen human biopsy specimens. High *miR-25-3p* expression in the pretreatment OS tissues was significantly correlated with poor overall survival ($p=0.004$, log-rank test; Fig. 1A). High *miR-25-3p* levels were also correlated with poor metastasis-free survival ($p=0.005$, log-rank test; Fig. 1B). The clinicopathological features of the patients in relation to the expression of *miR-25-3p* are summarized in Table 1. The statistical analysis revealed a significant correlation between high-*miR-25-3p* expression and the presence of metastasis ($p=0.014$) and the oncologic outcome ($p=0.003$). These data were consistent with those obtained previously for circulating *miR-25-3p* [12], indicating that both cellular and circulating *miR-25-3p* expression levels are significantly correlated with the prognosis of OS patients.

miR-25-3p regulates lethal phenotypes of OS cells. To investigate the role of *miR-25-3p* in OS cells, we performed a functional analysis by altering *miR-25-3p* expression. Because *miR-25-3p* was confirmed to be expressed at a higher level in OS cells compared to normal cells [12] (Fig. 2A), we performed functional analysis using locked nucleic acids (LNAs). LNA-antimiR-25-3p suppressed the *miR-25-3p* expression in OS cells (Fig. 2B). The proliferation assays revealed that *miR-25-3p* silencing suppressed the tumor growth ability in OS cells (Fig. 2C). In addition, cellular invasiveness was also reduced by LNA-antimiR-25-3p (Fig. 2D). Interestingly, *miR-25-3p* silencing improved the multidrug resistance in OS cells (Fig. 2E). These data revealed that *miR-25-3p* is a potential oncogenic miRNA in OS and contributes to the development of OS.

DKK3, a direct target of miR-25-3p, regulates cellular proliferation and invasion in OS. We screened the mRNA targets of *miR-25-3p* by using the *in silico* prediction algorithms miRanda, MiRtarget2 and TargetScan to determine the potential downstream pathway regulated by *miR-25-3p*. Among the 122 downstream targets of *miR-25-3p* revealed by both algorithms, *DKK3* was identified as a *miR-25-3p* target (Fig. 3A). *DKK3* plays an important role in the Wnt-β catenin signaling pathway, which is inactive in OS [13]. *DKK3* expression was inversely correlated with *miR-25-3p* in OS cells, confirming increased *DKK3* levels by *miR-25-3p* silencing (Fig. 3B).

To validate whether *DKK3* is regulated by *miR-25-3p*, we cloned the 3'UTR fragment containing the putative *miR-25-3p* binding site downstream of a luciferase coding sequence, and the luciferase reporter and *miR-25-3p* oligos were cotransfected into U2OS cells. The luciferase activity levels were approximately 72% lower in the cells cotransfected with *miR-25-3p* compared to the cells cotransfected with *miR-NC* oligos (Fig. 3C). We evaluated the functional consequences of silencing *DKK3* expression by using siRNA (Fig. 3D). Silencing

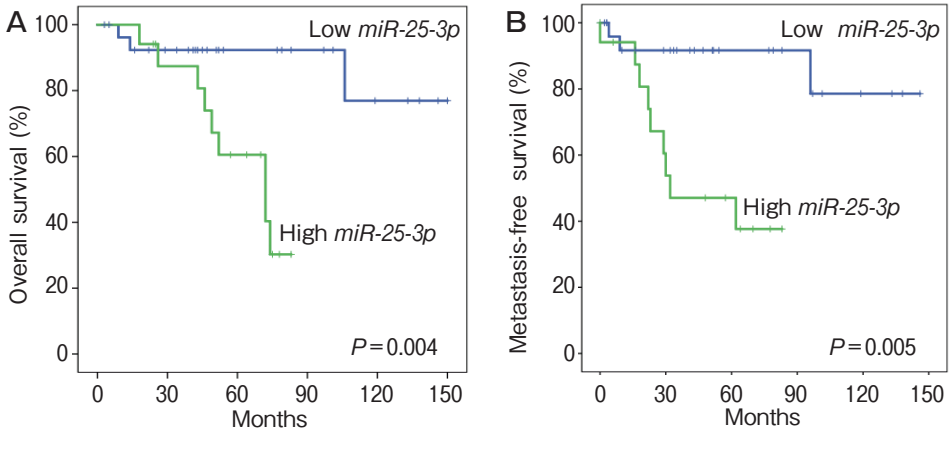

Fig. 1 Clinical relevance of *miR-25-3p* expression in OS. **A**, Kaplan-Meier survival curves for overall survival according to *miR-25-3p* expression (log-rank test, $p=0.004$); **B**, Kaplan-Meier survival curves for metastasis-free survival according to *miR-25-3p* expression (log-rank test, $p=0.005$).

the *DKK3* expression promoted the migration and invasion of the OS cells, but did not affect the drug resistance (Fig. 3E, F). Collectively, these results suggest that *DKK3*, a direct target of *miR-25-3p*, could act to prevent tumor growth and metastasis.

The DKK3 expression levels in the OS tissues were positively correlated with the patient prognosis. To determine the clinicopathological significance of *DKK3*, we performed a statistical analysis of the *DKK3* expression in OS tissues. Immunohistochemical staining revealed DKK3 to be diffusely positive in 55%, focally positive in 6%, and negative in 39% of the diagnostic incisional biopsy specimens, with DKK3 localized to the cytoplasm in the positive cases (Fig. 4A). The prognosis of the patients whose biopsy specimens were negative for DKK3 was poor, with 57% of these patients dying of the disease. Our Kaplan-Meier analysis of the RT-PCR results revealed that the *DKK3* expression levels were significantly correlated with the patients' prognoses. Low *DKK3* expression was significantly correlated with poor overall survival ($p = 0.022$, log-rank test) and poor disease-free survival ($p = 0.017$, log-rank test) (Fig. 4B, C). These data show the clinicopathological significance of *DKK3* to be inversely correlated with that of *miR-25-3p*, corresponding to the demonstrated functional relationship between *miR-25-3p* and its target.

Secretory miR-25-3p is embedded in OS-derived exosomes and mediates angiogenesis. We previously observed that *miR-25-3p* was released into the extracellular space in OS cells [12]. Here, to examine the delivery of secretory *miR-25-3p* into extracellular fluid, we purified tumor-derived exosomes and analyzed the *miR-25-3p* expression in exosome fractions. Scanning electron microscopy (SEM) revealed that the exosomes had a round shape with 40-100-nm-sized membrane vesicles (Fig. 5A). A nanoparticle tracking analysis of the purified exosomes revealed a fraction containing nanoparticles with a peak at 101 nm (Fig. 5B).

Our western blot analysis confirmed the expression of common exosomal surface markers, CD9 and CD81, in the exosome fractions (Fig. 5C). The RT-PCR revealed higher *miR-25-3p* expression levels in the tumor-derived exosome fractions compared to the exosome fractions from the hMSCs (Fig. 5D). These data suggest that secretory *miR-25-3p* in extracellular fluid may acquire stability via encapsulation by OS-derived exosomes. In addition, the capillary formation of HUVECs was significantly enhanced by the addition of OS-derived exosomes (Fig. 5E). Silencing of the *miR-25-3p* in HUVECs decreased the capillary formation; however, the addition of OS-derived exosomes restored the capillary formation in silenced HUVECs (Fig. 5F), suggesting that the transport of OS-derived exosomes containing *miR-25-3p* to endothelial cells may disrupt their microenvironment and promote OS development.

Finally, increased *miR-25-3p*

Table 1 Patient characteristics

Factor	No. of patients	*miR-25-3p* expression		*p*-value
		Low	High	
Age at diagnosis (yrs):				0.229
0–10	3	3	0	
11–20	16	8	8	
≥21	26	17	9	
Gender:				0.258
Male	20	14	6	
Female	25	14	11	
Location:				0.316
Femur	22	15	7	
Tibia	6	4	2	
Humerus	3	2	1	
Others	14	7	7	
Histological subtype:				0.398
Conventional	34	22	12	
Other	11	6	5	
Response to chemotherapy:				0.287
<90%	19	12	7	
≥90%	11	5	6	
Local recurrence:				0.538
Yes	7	4	3	
No	38	24	14	
Distant metastasis:				0.014
Yes	21	9	12	
No	24	19	5	
Oncologic outcome:				0.003
CDF/NED	26	21	5	
DOD	19	7	12	

CDF, continuous disease-free; NED, no evidence of disease; DOD, dead of disease.

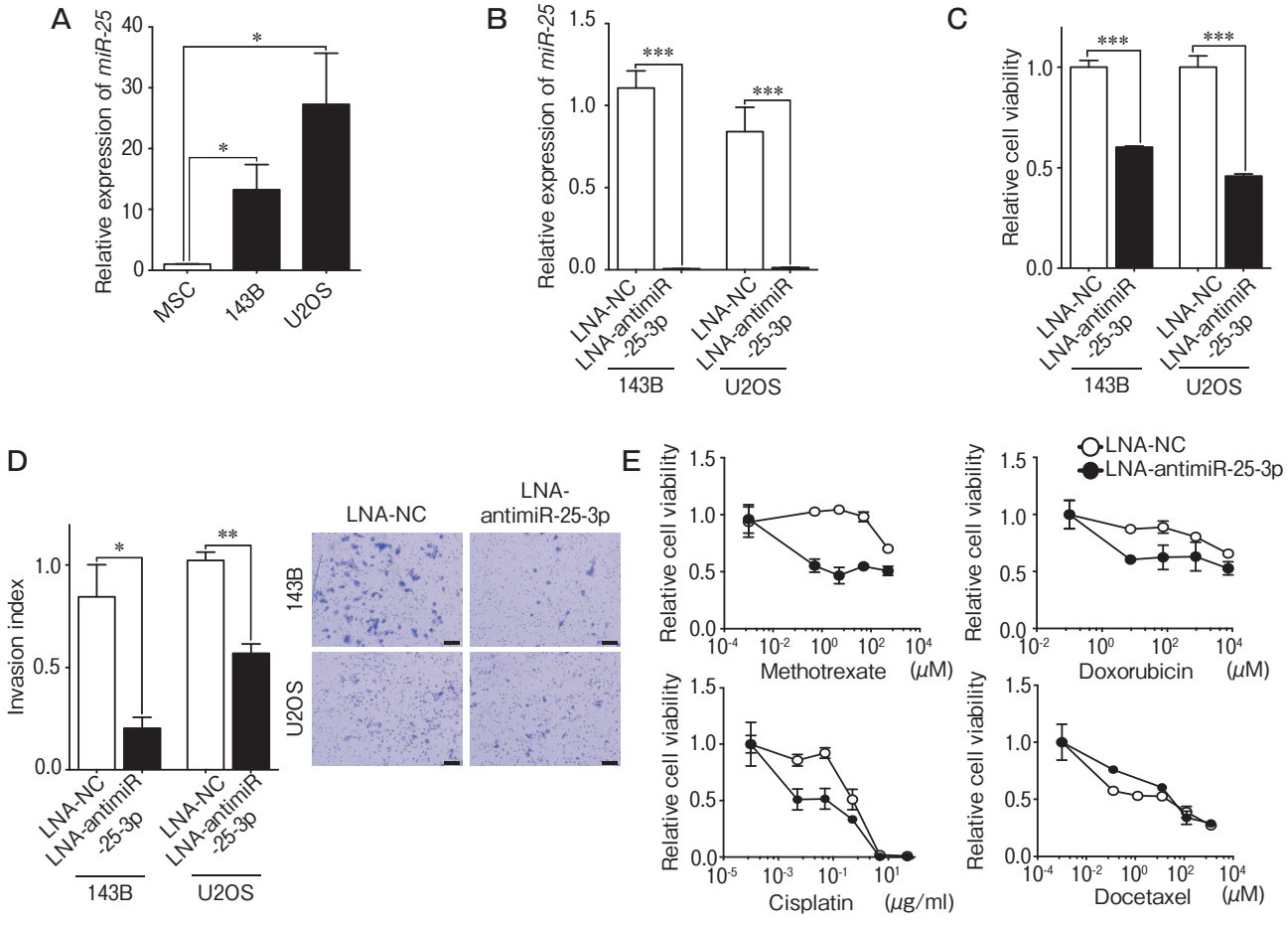

Fig. 2 *miR-25-3p* promotes OS cell proliferation, migration, and drug resistance. **A**, *miR-25-3p* expression levels in OS cells and human mesenchymal stem cells (hMSCs); **B**, *miR-25-3p* expression levels in OS cells after transfection with LNA scramble control (LNA-NC) or LNA-antimiR-25-3p; **C**, Relative proliferation rates of OS cells transfected with LNA-NC or LNA-antimiR-25-3p; **D**: Invasion analysis of OS cells treated with LNA-NC or LNA-antimiR-25-3p. Scale bar, 100 μm; **E**, Drug sensitivity according to *miR-25-3p* expression in the presence of methotrexate, doxorubicin, cisplatin, or docetaxel. Columns, mean of at least three independent experiments. Bars, SEM. $^{*}p<0.05$, $^{**}p<0.01$, $^{***}p<0.001$.

expression promoted the invasion and migration of HUVECs, whereas *miR-25-3p* silencing reduced these HUVEC phenotypes (Fig. 5G). These data suggest that extracellular miRNAs embedded in secretory exosome vesicles could be delivered to the tumor microenvironment and act as physiologically functional molecules to promote tumor progression.

Discussion

Accumulating evidence suggests that dysregulated miRNAs are involved in the oncogenesis, maintenance, and development of human malignant tumors [6, 7]. In addition, cell-free circulating miRNAs have been identified in patients with malignant tumors and may function in communication with the tumor microenvironment, indicating that they could be used as novel biomarkers in tumor diagnosis and monitoring [14]. However, few reports have addressed the clinicopathological significance and functional relevance of single dysregulated specific miRNAs in tumor development.

Ma and colleagues were the first to report an aspect of the functional significance of miRNAs by showing that the overexpression of a specific miRNA, *miR-10b*, contributed to the development of breast cancer metastasis [15]. In addition, oncogenic *miR-10b* secreted by breast cancer cells has been shown to suppress the protein level of its target genes, such as *HOXD10* and *KLF4*,

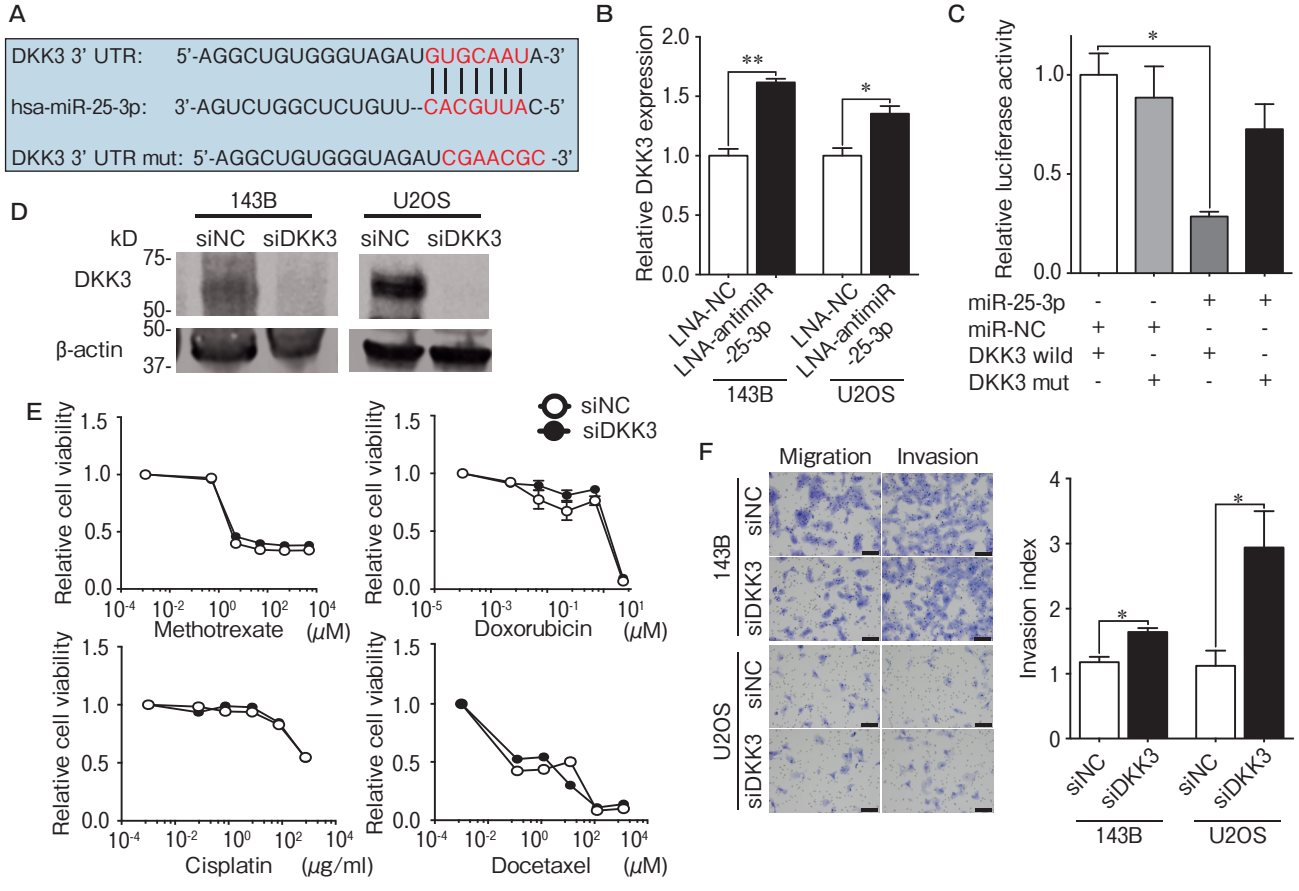

Fig. 3 Dickkopf-3 (*DKK3*) is a direct target of *miR-25-3p*. **A**, Alignments of *DKK3-3'UTR*, *hsa-miR-25-3p*, and *DKK3-3'UTR* mut, in which the complementary sites for the seed region of *miR-25-3p* are indicated; **B**, Relative *DKK3* expression in OS cells treated with LNA-NC or LNA-antimiR-25-3p; **C**, Luciferase activities of 143B cells co-transfected with *miR-25-3p* oligonucleotides and wild-type (wild) or mutant (mut) reporter vectors of *DKK3*; **D**, Western blot analysis of DKK3 expression after negative control siRNA (siNC) or siDKK3 transfection into 143B and U2OS cells, respectively; **E**, Drug sensitivity according to DKK3 expression in the presence of methotrexate, doxorubicin, cisplatin, or docetaxel; **F**, Invasion assays performed using 143B and U2OS cells at 24 h post-transfection with siNC or siDKK3. Scale bar, 100 μm. Columns, mean of at least three independent experiments. Bars, SEM. $^{*}p<0.05$, $^{**}p<0.01$.

in recipient cells, which can lead to a favorable environment for breast cancer development and progression [16]. However, *miR-10b* has rarely been reported to be present in the circulation and to have potential as a breast cancer biomarker. *miR-21*, an oncomiR, stimulates the invasion, intravasation, and metastasis of colorectal cancer [17]. Serum *miR-21* is a promising biomarker for the early detection and prognosis of colorectal cancer [18], but the extracellular function of *miR-21* in colorectal cancer is not fully understood. Our present findings demonstrated that *miR-25-3p* had functional and clinical significance in the intracellular and extracellular regions of OS cells and that it has a role in the promotion of tumor progression and development, suggesting that *miR-25-3p* could have potential as a diagnostic biomarker and a therapeutic target in OS patients.

We also observed that *miR-25-3p* affected not only the proliferative and invasive abilities of OS cells, but also their drug resistance. These phenotypes are consistent with the lethal phenotypes of tumor-initiating cells (TICs), which are designated cancer stem cells (CSCs). The hallmarks of TICs are not only their self-renewal ability, but also their resistance to conventional chemotherapeutic agents and high metastatic potential [19,20]. Recent studies have shown that miRNAs are associated with TIC phenotypes via their ability to simultaneously regulate their various target genes

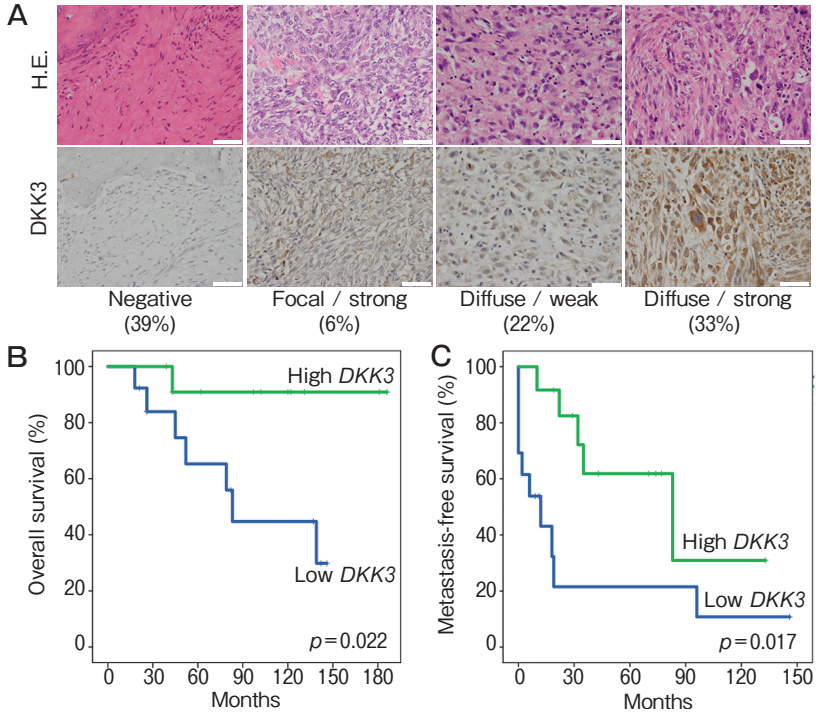

Fig. 4 Clinicopathological significance of DKK3 expression. **A**, Immunohistochemical staining of DKK3 and hematoxylin and eosin staining of OS biopsy specimens. Scale bar, 50 μm; **B**, Kaplan-Meier survival curves for overall survival according to *DKK3* expression (log-rank test, $p=0.022$); **C**, Kaplan-Meier survival curves for metastasis-free survival according to *DKK3* expression (log-rank test, $p=0.017$).

[21,22]. *miR-34a*, a p53 target, is reported to be a key negative regulator of prostate CSCs with a CD44-positive phenotype, which are responsible for the clonogenic expansion, tumor regeneration, and metastasis of prostate cancer [21]. In addition, let-7 is a master regulator of the $CD44^{+}/CD24^{-/low}$ cell population, a breast CSC fraction with a markedly high TIC [23].

Among these TIC phenotypes, the most important clinical phenotype is drug resistance. In the present study, we did not investigate the relevance of TICs in osteosarcoma; however, *miR-25-3p*, which can regulate drug resistance, could constitute a new therapeutic target for this cancer, and drugs targeting this miRNA could be used in combination with conventional therapeutic drugs. Since LNAs are currently undergoing phase II clinical trials for the treatment of hepatitis [24], it is to be expected that similar strategies could be used to develop miRNA therapeutics for the treatment of malignant diseases.

Several studies have demonstrated the contribution of exosomal miRNAs to cancer metastasis [25,26]. *miR-181c* promotes the destruction of the blood-brain barrier (BBB) by mediating the abnormal localization of actin via its ability to downregulate its target gene, *PDPK1* [26]. *miR-210*, which is released by metastatic breast cancer cells, is transported to endothelial cells via cancer-derived exosomes and suppresses the expression of specific target genes, resulting in enhanced angiogenesis [27]. In the present study, *miR-25-3p* was secreted by OS cells and induced the formation and migration of vascular endothelial cells. Although the effects of *miR-25-3p* have not yet been demonstrated *in vivo*, *miR-25-3p*, which is also upregulated in OS cells, altered the surrounding tumor microenvironment and stimulated tumor progression. The molecular mechanism linking OS-secreted exosomal *miR-25-3p* to the microenvironment of the lungs, a common site of distant metastasis, remains unclear and requires further exploration. A broad understanding of all of the functions of oncomiRs in tumor development will provide insights into how they could be used to develop new novel diagnostic and therapeutic approaches to malignant diseases.

Overall, our present findings demonstrate the clini-

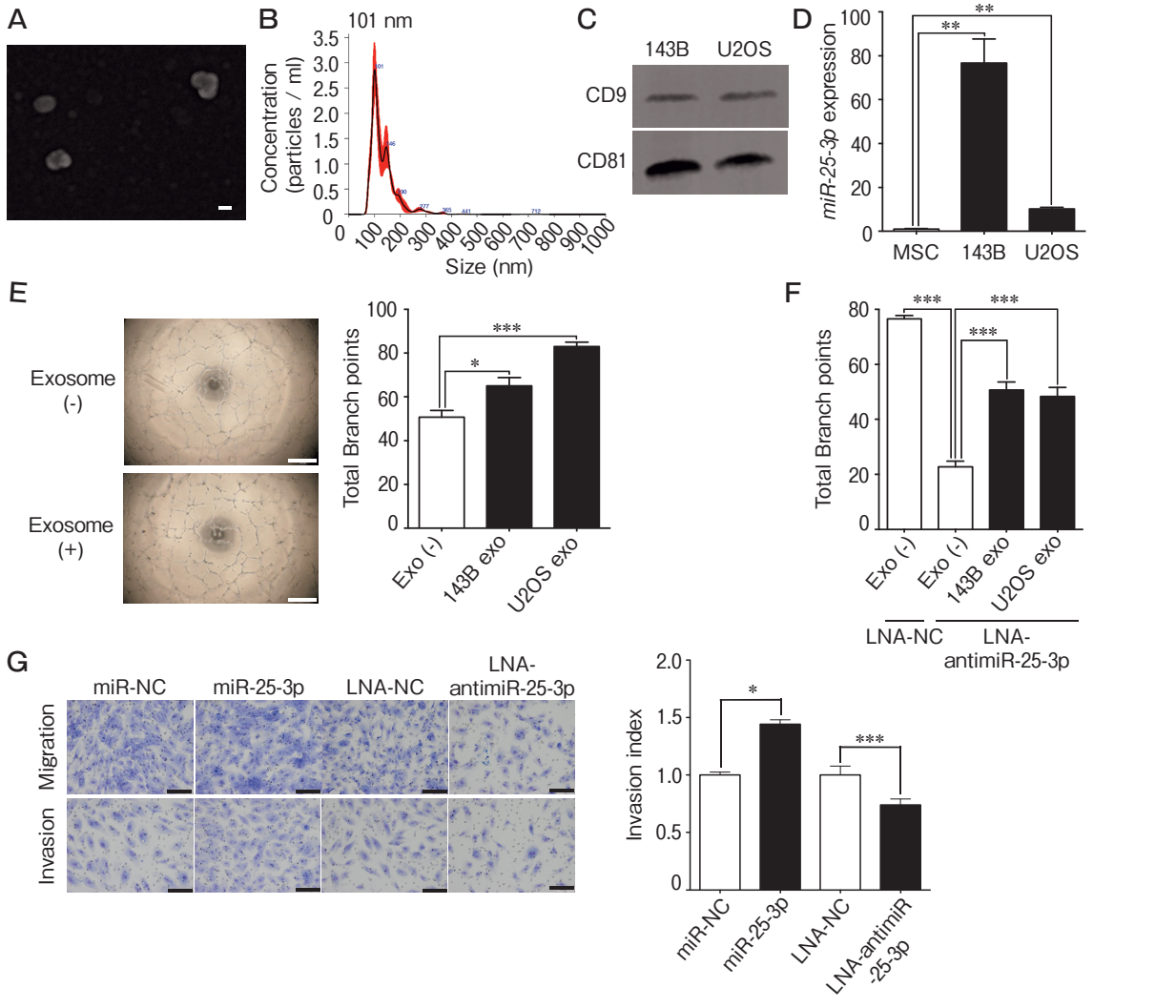

Fig. 5 Exosome-embedded secretory *miR-25-3p* affects function of normal vascular endothelial cells. **A**, SEM image of purified exosomes. Scale bar, 100 nm; **B**, Size distribution of exosomes assessed using the NanoSight® nanoparticle tracking system. The size range of isolated exosomes was approx. 40-200 nm, with a peak at 101 nm; **C**, Western blot of CD9 and CD81 in exosomes derived from 143B and U2OS cells; **D**, RT-PCR analysis of *miR-25-3p* expression in secreted exosomes derived from MSC and OS cells; **E**, HUVECs tube forming assay with or without exosomes derived from OS cells. Scale bar, 50 μm; **F**, Tube formation analysis with alteration of *miR-25-3p* expression and tumor-derived exosomes; **G**, Invasion analysis of HUVECs treated with mimic or LNA. Scale bar, 100 μm. Columns, mean of at least three independent experiments performed in duplicate. Bars, SEM. $^{*}p<0.05$, $^{**}p<0.01$, $^{***}p<0.001$.

copathological and functional significance of intracellular and extracellular *miR-25-3p* in OS. Intracellular *miR-25-3p* contributed to cellular proliferation, invasion, and drug resistance, which are lethal OS phenotypes. Extracellular *miR-25-3p*, which was enriched in OS-derived exosomes, was transported to endothelial cells and stimulated angiogenesis. The levels of circulating and intracellular *miR-25-3p* were significantly correlated with a poor prognosis in the present series of OS patients. By contrast, the expression of the Wnt signaling inhibitor *DKK3*, a *miR-25-3p* target, was correlated with a good prognosis in the OS patients. These findings contribute to our understanding of the intracellular and extracellular functions of dysregulated miRNAs in tumor biology and suggest that these functions could be analyzed in liquid biopsies and developed to provide novel therapeutics for OS patients.

Acknowledgments. We thank the member of the Central Research Laboratory of the Okayama University Medical School for the technical support for the isolation and validation of exosomes and histological analysis. The authors are supported by the Japan Orthopaedics and Traumatology Research Foundation (Grant no. 311), the Uehara Memorial Foundation, and JSPS KAKENHI Grants nos. 16K20054 and 16H05449.

References

1. Mirabello L, Troisi RJ and Savage SA: Osteosarcoma incidence and survival rates from 1973 to 2004. Cancer (2009) 115: 1531–1543.
2. Allison DC, Carney SC, Ahlmann ER, Hendifar A, Chawla S, Fedenko A, Angeles C and Menendez LR: A meta-analysis of osteosarcoma outcomes in the modern medical era. Sarcoma (2012) 2012: 704872.
3. Link MP, Goorin AM, Miser AW, Green AA, Pratt CB, Belasco JB, Pritchard J, Malpas JS, Baker AR, Kirkpatrick JA, Ayala AG, Shuster JJ, Abelson HT, Simone JV and Vietti TJ: The effect of adjuvant chemotherapy on relapse-free survival in patients with osteosarcoma of the extremity. N Engl J Med (1986) 314: 1600–1606.
4. Bartel DP: MicroRNAs: genomics, biogenesis, mechanism, and function. Cell (2004) 116: 281–297.
5. Kim VN, Han J and Siomi MC: Biogenesis of small RNAs in animals. Nat Rev Mol Cell Biol (2009) 10: 126–139.
6. Calin GA and Croce CM: MicroRNA signatures in human cancers. Nat Rev Cancer (2006) 6: 857–866.
7. Esquela-Kerscher A and Slack FJ: Oncomirs-microRNAs with a role in cancer. Nat Rev Cancer (2006) 6: 259–269.
8. Cortez MA, Bueso-Ramos C, Ferdin J, Lopez-Berestein G, Sood AK and Calin GA: MicroRNAs in body fluids—the mix of hormones and biomarkers. Nat Rev Clin Oncol (2011) 8: 467–477.
9. Schwarzenbach H, Hoon DS and Pantel K: Cell-free nucleic acids as biomarkers in cancer patients. Nat Rev Cancer (2011) 11: 426–437.
10. Valadi H, Ekstrom K, Bossios A, Sjostrand M, Lee JJ and Lötvall JO: Exosome-mediated transfer of mRNAs and microRNAs is a novel mechanism of genetic exchange between cells. Nat Cell Biol (2007) 9: 654–659.
11. Kosaka N, Iguchi H and Ochiya T: Circulating microRNA in body fluid: a new potential biomarker for cancer diagnosis and prognosis. Cancer Sci (2010) 101: 2087–2092.
12. Fujiwara T, Uotani K, Yoshida A, Morita T, Nezu Y, Kobayashi E, Yoshida A, Uehara T, Omori T, Sugiu K, Komatsubara T, Takeda K, Kunisada T, Kawamura M, Kawai A, Ochiya T and Ozaki T: Clinical significance of circulating miR-25-3p as a novel diagnostic and prognostic biomarker in osteosarcoma. Oncotarget (2017) 8: 33375-33392.
13. Cai Y, Mohseny AB, Karperien M, Hogendoorn PC, Zhou G and Cleton-Jansen AM: Inactive Wnt/s-catenin pathway in conventional high-grade osteosarcoma. J Pathol (2010) 220: 24–33.
14. Schwarzenbach H, Nishida N, Calin GA and Pantel K: Clinical relevance of circulating cell-free microRNAs in cancer. Nat Rev Clin Oncol (2014) 11: 145–156.
15. Ma L, Teruya-Feldstein J and Weinberg RA: Tumour invasion and metastasis initiated by microRNA-10b in breast cancer. Nature (2007) 449: 682–688.
16. Singh R, Pochampally R, Watabe K, Lu Z and Mo YY: Exosome-mediated transfer of miR-10b promotes cell invasion in breast cancer. Mol Cancer (2014) 13: 256.
17. Asangani I, Rasheed S, Nikolova D, Leupold J, Colburn N, Post S and Allgayer H: MicroRNA-21 (miR-21) post-transcriptionally downregulates tumor suppressor Pdcd4 and stimulates invasion, intravasation and metastasis in colorectal cancer. Oncogene (2008) 27: 2128–2136.
18. Toiyama Y, Takahashi M, Hur K, Nagasaka T, Tanaka K, Inoue Y, Kusunoki M, Boland CR and Goel A: Serum miR-21 as a diagnostic and prognostic biomarker in colorectal cancer. J Natl Cancer Inst (2013) 105: 849–859.
19. Dean M, Fojo T and Bates S: Tumour stem cells and drug resistance. Nat Rev Cancer (2005) 5: 275–284.
20. Clevers H: The cancer stem cell: premises, promises and challenges. Nat Med (2011) 17: 313–319.
21. Liu C, Kelnar K, Liu B, Chen X, Calhoun-Davis T, Li H, Patrawala L, Yan H, Jeter C, Honorio S, Wiggins JF, Bader AG, Fagin R, Brown D and Tang DG: The microRNA miR-34a inhibits prostate cancer stem cells and metastasis by directly repressing CD44. Nat Med (2011) 17: 211–215.
22. Fujiwara T, Katsuda T, Hagiwara K, Kosaka N, Yoshioka Y, Takahashi RU, Takeshita F, Kubota D, Kondo T, Ichikawa H, Yoshida A, Kobayashi E, Kawai A, Ozaki T and Ochiya T: Clinical relevance and therapeutic significance of microRNA-133a expression profiles and functions in malignant osteosarcoma-initiating cells. Stem Cells (2014) 32: 959–973.
23. Yu F, Yao H, Zhu P, Zhang X, Pan Q, Gong C, Huang Y, Hu X, Su F, Lieberman J and Song E: let-7 regulates self renewal and tumorigenicity of breast cancer cells. Cell (2007) 131: 1109–1123.
24. Li Z and Rana TM: Therapeutic targeting of microRNAs: current status and future challenges. Nat Rev Drug Discov (2014) 13: 622–638.
25. Tominaga N, Kosaka N, Ono M, Katsuda T, Yoshioka Y, Tamura K, Lötvall J, Nakagama H and Ochiya T: Brain metastatic cancer cells release microRNA-181c-containing extracellular vesicles capable of destructing blood-brain barrier. Nat Commun (2015) 6: 6716.
26. Zhang L, Zhang S, Yao J, Lowery FJ, Zhang Q, Huang WC, Li P, Li M, Wang X, Zhang C, Wang H, Ellis K, Cheerathodi M, McCarty JH, Palmieri D, Saunus J, Lakhani S, Huang S, Sahin AA, Aldape KD, Steeg PS and Yu D: Microenvironment-induced PTEN loss by exosomal microRNA primes brain metastasis outgrowth. Nature (2015) 527: 100–104.
27. Kosaka N, Iguchi H, Yoshioka Y, Takeshita F, Matsuki Y and Ochiya T: Secretory mechanisms and intercellular transfer of microRNAs in living cells. J Biol Chem (2010) 285: 17442–17452.